WOOD RESEARCH
64 (3): 2019
423-436

MECHANICAL PROPERTIES AND MICROSTRUCTURE OF *ZABELIA BIFLORA*

Liangfei Gong, Qingming Zhang, Haozhe Liang, Siyuan Ren
Beijing Institute of Technology, State Key Laboratory of Explosion Science and Technology
Beijing, China

Qingming Zhang, Jie Wang
Beijing Institute of Technology, Department of Mechanics
School of Aerospace Engineering
Beijing, China

(Received June 2018)

ABSTRACT

Zabelia biflora, a kind of broad-leaved shrub, with six distinct longitudinal furrows and petal-like structure in cross section, belongs to *Zabelia* and consists of sections interlaced with each other. It is meaningful to focus on the peculiar appearance of *Zabelia biflora* for the sake of outstanding structures. On the basis of quasi-static experiments of stretching, compression along the grain direction and bending in the tangential direction, dynamic experiments of the wood over its water contents ranging from 9% to 22% have been investigated using the split Hopkinson pressure bar. Combined with the electron scanning, 3D X-ray scanning reveals the microstructure of *Zabelia biflora*. Results show that the maximum bending force of this wood on the joint is higher than that of wood without the joint. Besides, although the static mechanical parameters of *Zabelia biflora* are basically the same order of magnitude compared with other hardwoods, the bending strength of the specimen with a joint is significantly improved by contrast with the wood possessing a similar density with it. In addition, it is been proved that there is a symmetrical and glass-like density distribution in the center of the wood. Meanwhile, the density presents a gradient-layer distribution from the up-down view. The dynamic compression strength of the wood will decrease when the water content ascends at every strain rate. When the strain rate is relatively low, the compression strength will rise abruptly with the descent of the moisture content below the fiber saturation point, otherwise, this enhancement will be slower. Moreover, the strain rate exerts a reinforcement effect on the compression strength. It is not until the strain rate exceeds 1000 s^{-1} that there will be a sudden drop in the stress after the first arrival of the compression strength. The influence of the moisture content on dynamic platform stress of material matters only under low strain rates. Once the moisture content is higher than the fiber saturation point, this effect will also disappear.

KEYWORDS: *Zabelia biflora*, quasi-static experiments, dynamic experiments, 3D X-ray scanning.

INTRODUCTION

With the rapid advance of materials science and technology, people are capable of designing various kinds of materials that can meet higher requirements for the engineering application in the field of medicine, aerospace, military etc. It is an eternal matter needing to be considered to attain an appropriate balance between strength and toughness when developing new materials (Ritchie 2011), which entirely depends on the purpose of those materials. In the early time, people directly aims to utilize those natural materials evolving for hundreds of years or even longer. But subsequently those materials no longer satisfy their demands, leading to the generation of bionic science (Wegst et al. 2014), a study of the relationship between intrinsic microstructures of biological materials and extrinsic mechanical parameters inspired by the extraordinary macroscopic mechanical properties of many creatures in nature, such as higher ratio strength, higher ratio rigidity, and excellent ability of energy absorption and self-repair (Sun and Bhushan 2012, Pan 2014, Gao et al. 2003). It is of great significance to pay attention to these natural materials especially for the biomimetic synthesis of the functional material. As natural and renewable materials, woods are widely used due to the high ratio intensity and dissipation of abundant energy. On the one hand, they can be directly employed as building materials and protection structures of the spacecraft. In addition, their hierarchic structures ranging from micro-fibril arrangements (nanometer) to pore distributions (micrometer) are often regarded as the vital enlightenment of composites and absorption materials where the fracture toughness has been greatly improved (Jeronimidis 1980, Gordon et al. 1980, Fratzl and Weinkamer 2007). Thanks to the tremendous progress made in experimental technology, the nanoscale plane structure of wood can be observed by the scanning electron microscope (SEM) and transmission electron microscope (TEM) (Borrega et al. 2015, Allison et al. 2013). With the spectrum analysis (Tsuchikawa and Kobori 2015, Park et al. 2013), X-ray scanning and reconstruction available to three-dimensional structure of wood (Sakellariou et al. 2004, Mayo et al. 2010), 3D printing technology provides a convenient and possible way to the production of materials possessing complex structures (Wegst et al. 2014, Gu et al. 2016, Duigou et al. 2016, Dimas et al. 2013).

The major focuses of researchers about the wood can be roughly classified into two aspects and the first categories are hierarchic structure and its connection with the macroscopic mechanical behavior. Reiterer et. al (1999) studied the spiral arrangement of cellulose fibers on the secondary cell wall in European spruce by X-ray diffraction. Fratzl and Weinkamer (2007) summarized the tubular wall structure of the spruce and revealed the relationship between the angle arrangement of the microfibril and the distance to the pith, the angle distribution and the elastic modulus, the angle and the fracture strain in the early and late wood, respectively. Mayo et al. (2010) analyzed the impact of the X-ray microtomography on the attainment of the microstructure of the wood and reconstruction especially for obtaining images with high quality and resolution. Park et al. (2013) gained the content of crystalline cellulose in Arabidopsis using sum frequency vibration spectrum. Borrega et al. (2015) acquired cell wall structures of the balsa by SEM and X-ray diffraction and subsequently explained that the prominent mechanical performance per mass of the wood derived from the low laying angle of microfibrils and high cellulose crystallinity. Others also figured out that the high rupture work of unit mass compared with the steel and many man-made composite materials came from the unrecoverable plastic work, which is closely

related to the spiral angle distribution of the secondary cell wall (Jeronimidis 1980, Gordon et al. 1980). Besides, experimental investigations and theoretical analysis on responses of some particular woods to the static and dynamic loading were achieved. Rosyk et al. (2013) studied the static tensile performance of microtome samples of pine wood. Renaud et al. (2010) took the effect of the liquid on the dynamic compressive strength of three kinds of woods into account and mentioned that the density, temperature plus the strain rate mattered in the fracture. Reid and Peng (1997) made a respective explanation to the deformation mechanism of the wood under the uniaxial static and dynamic compression after the corresponding experiments. Müller et al. (2003) described the differences in mechanical properties between the moist wood after drying and native humid wood as well as failure modes under various loadings. Vural and Ravichandran (2003) carried out dynamic experiments of woods with different densities using the split Hopkinson bar and deduced a theoretical modeling for the dynamic deformation. Goodrich et al. (2010) discussed the thermal softening and the cooling phenomena of balsa. Caré et al. (2012) noted that the deformation is not uniform in the early and late wood owing to the different water contents and grasped the relationship between the expansion strain and moisture content. Adler and Buehler (2013) established a universal theoretical model associated with the angle of microfibrils to depict the axial mechanical properties of the cell wall and verified it with experimental results. Kránitz et al. (2014) tested the dynamic elastic and shear modulus of the old lumber using the ultrasonic instrument and found it out that the dynamic modulus is anisotropic and the relationship between the modulus and density in the old wood was the same as that of the new one. Startsev et al. (2015) paid attention to the effects of wood water content on dynamic shear strength and demonstrated that the glassy phase change and decomposition temperature of the wood remained the same whether in wet or dry wood.

Zabelia biflora gained interests of researchers primarily because of the special appearance. Ogata (1991) caught the microscopic characteristics of *Zabelia biflora* through comparisons of the microscopic section anatomy of branches and stems with that of other specimens in the same genus. Jacobs et al. (2011) analyzed the provenance of *Zabelia biflora* by combining the molecular structure of the tree and morphological features of fruits and seeds. But so far, most of the researchers intend to study the kinship of *Zabelia biflora* from the perspective of botany. This paper first paid attention to the static and dynamic mechanical performance of *Zabelia biflora*. With the consequences of X-ray 3D scanning, the microscopic structure of this wood is determined.

MATERIALS AND METHODS

Macrostructure and composition of the *Zabelia biflora*

The wood selected in this paper is shown in Fig. 1. *Zabelia biflora* belonging to the genus of *Zabelia* and the honeysuckle family, perennial broad-leaved shrub, grows much slowly (Ogata 1991). Due to the fact that most cells and tissues of the wood are parallel to the trunk, arranged along the axial direction and the main cells are concentric, this wood can approximately be considered as the orthotropic material. Along the grain direction, *Zabelia biflora* consists of sections interlaced with each other. Each section has a length of 10-15 cm and owns six distinct longitudinal furrows converging to the pith, which can be clearly seen from the cross section. The cartesian coordinate systems are finally defined as the axial direction along the grain, the radial direction parallel to the cross section, and the tangent direction perpendicular to both directions.

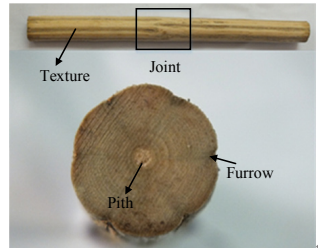

Fig. 1: Macroscopic features of Zabelia biflora.

Preparation of specimens

Since the peculiar joint structure of *Zabelia biflora*, it can be boldly guessed that this has something to do with the outstanding mechanical performance. In order to confirm our conjecture, experimental preparations are made. Firstly, raw materials with and without the joint are respectively selected. Then, to ensure that a uniform static mechanical characteristic can be received, specimens should cover all areas from the pith to the bast, with one part close to the pith and the other far away from the pith shown in Fig. 2.

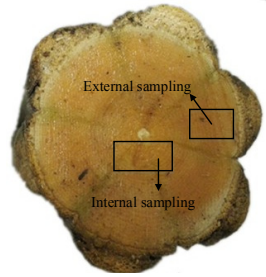

Fig. 2: Material selection in cross direction of experimental specimens.

Lastly, the water content should be strictly controlled and measured before the static and dynamic experiments because of the unneglectable effect of moisture content on the strength of the wood (Oloyede and Groombridge 2000). The natural and artificial drying methods are commonly adopted in the wood drying, and the disadvantage of the former is obviously witnessed by the long cycle. So, the extreme efficient vacuum drying which can provide specimens with high qualities is introduced in our experiments. After a number of samples with dimensions of 20 x 20 x 20 mm being captured from the two types of raw materials mentioned above, the mass of each specimen is recorded as m_1 before the test. Then the vacuum value and temperature are set to -0.07 MPa and 50°C, respectively. It is not until all samples reach dried that the measurement is accomplished (if the difference between the last two weighing is no more than 5%, the sample is thought to be dried). In the end, the dried weight of the sample can be marked as m0. The moisture content w can be accordingly calculated by the following Eq. 1:

$$w = \frac{m_1 - m_0}{m_0} \times 100 \quad (\%) \tag{1}$$

Therefore, the moisture content fit for experiments can be arbitrarily controlled by monitoring the mass of each specimen every 1 h or 2 h. In our experiments, the water contents are adjusted to be in a range of 8% ~ 13% for static experiments and 8% ~ 22% for dynamic tests.

It should be emphasized that the final moisture content in the experimental result is determined after each test.

After the water contents of small specimens with dimensions of 20 x 20 x 20 mm being adjusted to be dried and 12%, respectively, the corresponding density of 0.76 g·cm^{-3} and 1.07 g·cm^{-3} in these two moisture contents are acquired.

Due to the little knowledge about the basic mechanical quantities of *Zabelia biflora*, the quasi-static tensile and compression experiments are conducted involving in the axial tensile strength, axial elastic modulus and compressive strength along the grain. Compressive samples are made up of small cuboids of 10 x 10 x 15 mm, and the longer side points to the axial direction. Specimens used in the bending experiments are still cuboids of 10 x 10 x 150 mm. It should be paid extra attention that all specimens mentioned above plus the stretching samples should contain two categories including the joint and without the joint.

Moreover, bending experiments of two kinds of raw *Zabelia biflora* with the length of 150 mm are added. Specimens for dynamic experiments are processed into standard cylinders with a diameter of 7 mm and a height of 5 mm.

Static mechanical performance

Axial stretching and compression

Static experiments are mainly implemented using the material testing machine (MTS). The experimental temperature is about 24°C, and the moisture content is 11%. As is shown in Fig. 3a, an extensometer with a range of 50 mm is applied to measure the displacement of the effective segment of the tensile specimen.

The fixture should be checked before the experiment to prevent the measurement error caused by the looseness, and it is should be guaranteed that the texture is parallel to the center line.

According to the relationship between the load and deformation within the proportionality limit, the elastic modulus of the longitudinal grain can be computed by fitting the relationship between the force and deformation of each loading (Eq. 2), and the final consequence is averaged by results of multiple tests.

$$E_n = \frac{\Delta\sigma}{\Delta\varepsilon} = \frac{l}{A} \times \frac{\Delta p_n}{\Delta l_n} \quad \text{(MPa)} \tag{2}$$

where: n - represents the n-th loading,
E_n - the elastic modulus of the n-th loading (MPa),
Δp_n - stands for the force difference between the upper and lower limit (N),
Δl_n - the difference between the final and the initial displacement (mm),
l - denotes the effective length of the specimen (mm),
A - cross-sectional area of the specimen (mm^2).

The tensile strength is given as follows:

$$\sigma_w = \frac{p_{\max}}{bt} \quad \text{(N)} \tag{3}$$

where: p_{max} - the failure force (N),
b - the width of the specimen (mm),
t - the thickness of the specimen (mm).

As is depicted in Fig. 3b, when specimens are subjected to the tensile loads, they will break from the part with relatively fewer fibers because of the uneven distribution of fibers. On the contrary, the damaged section will be more orderly shown in Fig. 3c.

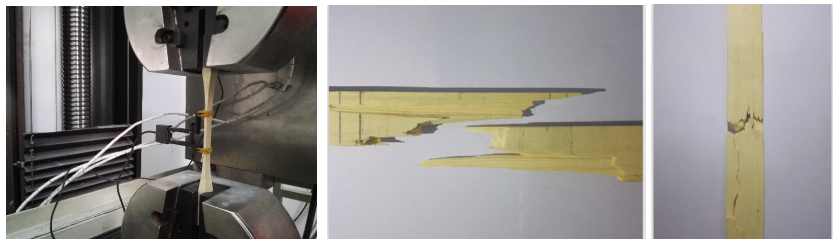

(a) (b) (c)

Fig. 3: Axial tensile tests. (a) The experimental process. (b) Tear failure of the fibers. (c) Transverse fracture failure.

The formula of compressive strength is the same as that of the stretching (Eq. 3). It can be seen that three main types of compression failures are successively displayed in Fig. 4. From left to right, they are the external expansion, buckling and 45° shear failure, respectively. In general, the percentage of the matrix and fiber affects the damage forms. When the content of the matrix is low, the outer expansion of the specimens will appear because of the force beyond the tensile limit. On the other hand, the buckling is caused by the lack of the protection of the matrix when fibers are compressed; however, the shear failure will happen owing to the reach of the shear failure strength when the matrix bears the compression.

Fig.4: Compression failure modes in the grain direction.

Tangential bending

Given the fact that the mechanical performance of most woods in the axial direction is superior to that of the other two directions and the sectional dimension limit of *Zabelia biflora*, the experiments in the tangential direction are only considered. Furthermore, it is important to note that only the comparison of the maximum force between the raw *Zabelia biflora* materials with and without joints is taken into account in our study. The bending modulus and strength derived from the three-point bending methods displayed in Fig. 5 can be obtained as follows:

$$E_w = \frac{\Delta p l^3}{4 \Delta f b h^3} \quad \text{(MPa)} \tag{4}$$

$$\sigma_w = \frac{3 p_{max} l}{2 b h^2} \quad \text{(MPa)} \tag{5}$$

where: w - presents the moisture content (%),
E_w - the bending modulus (MPa),
σ_w - the bending strength (MPa),
Δp - the difference between the upper and lower force (N),
p_{max} - stands for the failure force (N),
Δf - the deflection increment (mm),
l - the span (mm),
b and h - the width and the height of the specimen, respectively (mm).

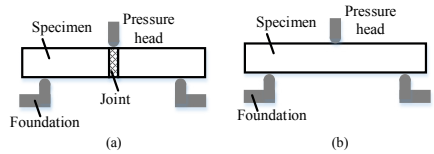

Fig. 5: Diagram of the three-point bending experiment in the tangential direction. (a) Specimens with the joint. (b) Specimens without the joint.

D X-ray scanning

Fig. 6 describes the imaging principle of the 3D X-ray scanning. The whole system is characterized by the combination of the traditional geometrical and optical amplification, in which the requirement of the resolution for the observer can be achieved without the sample being infinite close to the light source, and its maximum spatial resolution can reach to the nanometer. Similar to the theory of a microscope, the principle of the optical amplification can be reported as the following process where the continuous visible light, transformed by the scintillator when X-ray passes through it, firstly can be amplified by the high-resolved coupled lens detector, and then the amplified images will be presented through the camera after the process of photoelectric conversion. So, the magnification of the 3D X-ray microscope expressed as the product between the geometric and the optical magnification is dramatically enhanced. During the experiment, the distance between the specimen and the X-ray source is adjusted according to the size of the specimen and the expected resolution. To optimally match the X-ray energy and the sample, the filter plate is subsequently adopted based on the density of the specimen. When all preparations are ready, the scan can finally start.

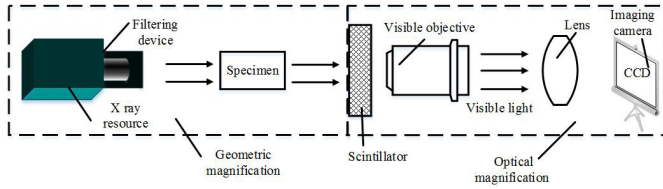

Fig. 6: Schematic diagram of imaging principle of the X-ray 3D scanning microscope.

Dynamic mechanical performance

The dynamic compression experiments are carried out on the alloy steel Hopkinson pressure bar with a diameter of 14.5 mm, and the loading and measurement systems are exhibited in Fig. 7.

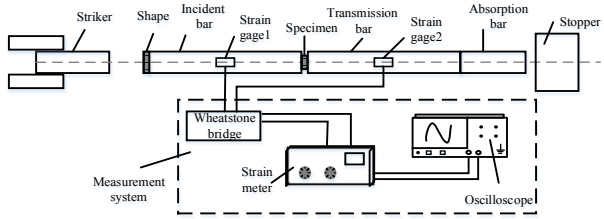

Fig. 7: Schematic of the Hopkinson pressure bar of alloy steel (diameter of 14.5 mm).

On account that *Zabelia biflora* is the porous material with low density, problems of the small transmitted signal, multiple loadings and the dissatisfaction of the assumption of the stress uniformity should be tackled with when using this compression system. Generally, they can be solved by the experimental technology. On the one hand, the semiconductor strain gauge and the pulse shaper are usually used. The former is fixed on the transmission bar because of its higher sensitivity than that of the resistance strain gauge, and the latter is applied to increase the rise time of the incident wave thanks to the good plasticity, which can not only solve the problem of stress equilibrium at both ends of the specimen but also can realize the constant strain rate loading. On the other hand, more metal bars with lower wave impedances can be introduced, such as aluminum or polymer rods and so on. The first one method is mainly considered in our tests, in which the brass plate with a thickness of 1mm and diameter of 4 mm is pasted by vacuum grease on the front end of the incident bar. To reduce the frictional effect caused by the roughness of the ends of specimens, the surfaces of them are smoothed with the fine sandpaper before the experiments. The transformation system of the strain signals is composed of the Wheatstone bridge and the dynamic strainmeter, which are finally recorded by the oscilloscope. In our experiments, the real stress-strain relationships of the wood owning different moisture contents at various strain rates are captured.

RESULTS AND DISCUSSION

The comparisons of the maximum bending force between dried specimens with and without joints are demonstrated in Tab. 1, in which only the No. 1, No. 2, and No. 3 samples possess joints. The equivalent diameter is signified as the inscribed circle diameter of *Zabelia biflora* in the cross section. It can be revealed that unlike the mean maximum stress of 11.3 MPa that the specimens with joints sustain, the maximum stress is relatively smaller for samples do not have joints. Specifically, compared with the maximum force of the No.4 specimen, the averaged force of specimens with joints is notably promoted by 30%, which powerfully indicates that the joint does have a positive effect on the bending performance of *Zabelia biflora*. Thus it is reasonable to connect this fantastic trait with the microstructure.

Tab. 1: Comparisons of maximum bending force between specimens with and without joints.

Specimens	With a joint	Water content	Equivalent diameter (mm)	Maximum force (N)	Maximum stress (MPa)
1	yes	dry	14.36	1829	11.30
2	yes	dry	14.32	1850	11.49

3	yes	dry	13.74	1682	11.35
4	no	dry	12.10	1000	8.70
5	no	dry	13.22	1279	9.26

As evidently is illustrated in Tab. 2 that the compressive strength, bending strength and modulus of *Zabelia biflora* are basically the same order of magnitude compared with other hardwoods. Each mechanical property in the axial direction is given as one value in those specimens with and without the joint exhibit the same features, however, the performance described in Tab. 1 in the tangential direction makes a difference. Concretely, from the contrast with the Bubinga possessing a similar density with *Zabelia biflora*, the bending strength is significantly improved by 19.66%, leading to a guess of the relation to the unique microstructure of the joint.

Tab. 2: Comparison of the static mechanical performance.

Tree species	Density ($g \cdot cm^{-3}$)	Water content (%)	Axial direction		Tangential direction (with a joint)	
			Tensile modulus	Compression strength	Bending modulus	Bending strength
Zabelia biflora	0.93-1.07	13	8182	59.1	10789	141.2
Rosewood	>0.769	12	18627	59.8	16873	177
Red rosewood	>0.85	12	19610	58.2	16150	232
Bubinga	0.88-1.10	12	15236	59.8	8415	118

From the speculation mentioned above, we then devote to uncovering the scanning structure of *Zabelia biflora* containing the joint (Fig. 8). In Figs. 8a and 8b, a symmetrical and glass-like density distribution can be clearly seen in the center of the scanning region where the density of the joint is higher than any other parts. From the top to the bottom depicted in Figs. 8b and 8c, it can be concluded that there is an obvious stratified density distribution, which is another distinct feature from other woods.

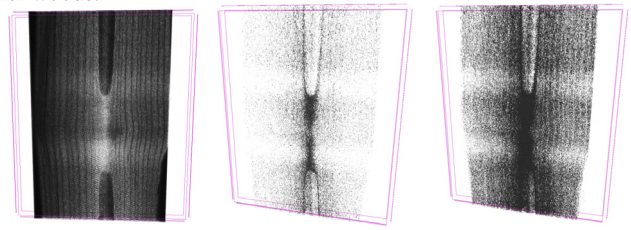

(a) (b) (c)

Fig. 8: 3D scanning results of specimens with joints: (a) The middle part of the picture denotes the joint region (the darker parts indicate the lower density), (b) Symmetrical glass-shaped density structure (the darker parts indicate the higher density), (c) The layer-shaped density distribution around the joint region (the darker parts indicate the higher density).

Unlike the negative role of the knot played in the connection of branch and trunk reported by Baño et al. (2013) and Foley (2003), the promoting bending effects of the joint, locating in center places between trunks, are reasonable thanks to the characteristic of density distribution. A similar gradient-oriented distribution is also emphasized surrounding in knots by Buksnowitz et al. (2010).

The relationships between the axial dynamic compression strength of *Zaeblia biflora* and the moisture content subjected to various strain rates are reflected in Fig. 9. Because of the little differences of the dynamic mechanical properties in the axial direction displayed between the specimens with and without the joints, the results are not distinguished according to the category of the samples. In general, the dynamic compression strength will decrease with the increase of the water content under each strain rate. Particularly, if the moisture content is below the fiber saturation point (11% - 12%), the compression strength will rise promptly with the decrease of the moisture content when the strain rate is low (less than 3000 s^{-1}), while when strain rate is higher, this enhancement will be slower. Hence, it is very necessary to control the moisture content of every specimen before the dynamic tests.

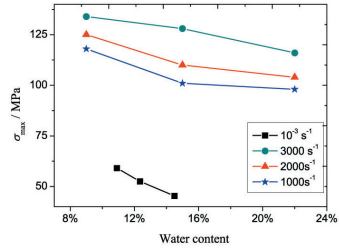

Fig. 9: The effect of moisture content on compressive strength.

As shown in Fig. 10, the strain rate exerts a reinforcement effect on the compression strength when the moisture is kept unvaried. When the strain rates equal 450 s^{-1} and 1000 s^{-1}, respectively, no significant differences between the strength and the flow stress are observed.

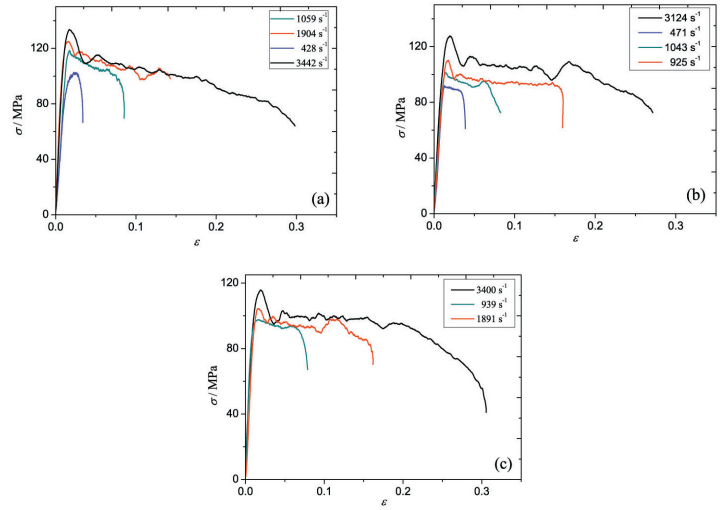

Fig. 10: The effect of strain rate on the compressive process: (a) 9%, (b) 15%, (c) 22%.

However, if the strain rate is improved further, there will be a sudden drop of the stress after the first arrival of the compression strength until the stress reaches the platform stress, which is associated with the inertia effect of the microstructure of the material. When the wood is fast compressed, the bending and twisting belt will form in the most vulnerable place of wood cells,

resulting in the localized rigidification representative of the increase of the compression strength. After the local wood cells collapse, the strength of the surrounding cells will be weakened, and thus the platform stress will naturally descend.

As is reported by Vural and Ravichandran (2003), when the strain rate is high, the dynamic pressure of soft wood is experiencing a transformation of peak to platform as well, the difference lies in that the peak pressure of *Zabelia biflora* is one to two times of the soft wood.

Fig. 11 illustrates the influences of the moisture content on the compressive curve of the relationship between the stress and the strain.

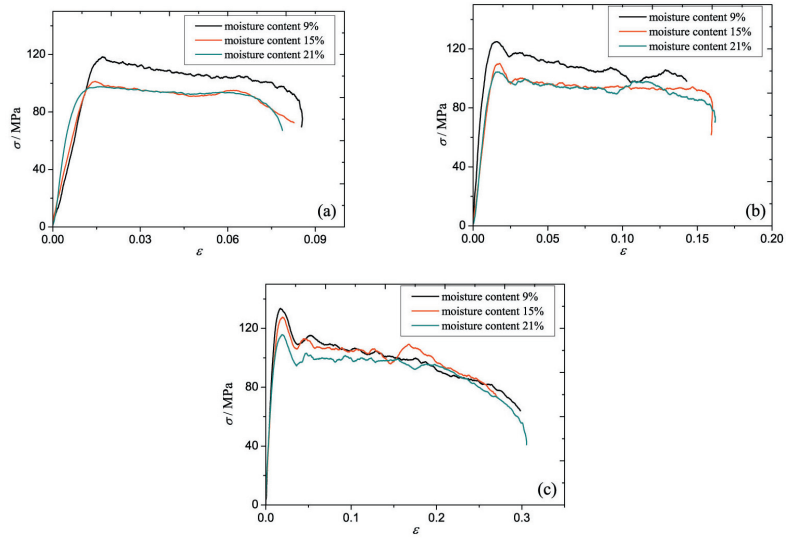

Fig. 11: The effect of moisture content on the compressive process: (a) 1000 s^{-1}, (b) 2000 s^{-1}.

It can be summarized that though there exits an observable difference of the platform stress between water contents below and beyond the fiber saturation point under low strain rates (1000 s^{-1} and 2000 s^{-1}), the distinction of the platform stress in higher strain rate (3000 s^{-1}) is not so obvious no matter how much water the sample has, that is, the force applied to produce the continuous deformation is basically the same in higher strain rate, which verifies that the effect of the moisture content on the dynamic yield strength of the material is so small that can be neglected in extreme high strain rate. In addition, the platform stress almost stays invariable when the moisture content exceeds the fiber saturation point in lower strain rates (Figs. 11a and 11b), so, the high moisture contents have little effect on the dynamic yield strength in this case.

CONCLUSIONS

Considering that the *Zabelia biflora* always grows in the windy places, like the north region in China, its specific appearance may have some relation to its abilities to resist the bending and so on. Furthermore, little has been known about the mechanical performance of this wood. In this paper, preliminary explorations about the static, dynamic mechanical properties and the microstructure of *Zabelia biflora* have been made. The results are proposed as follows:

1) Compared with the specimens without the joints, the samples owning the joints can bear a bigger bending force more than 30%. Although the static mechanical parameters including the compressive strength, bending strength and modulus, have the same order of magnitude as those of other common hardwoods, the bending strength of the sample with a joint can be significantly improved by 19.66% by contrast with the Bubinga, which possesses a similar density with *Zabelia biflora*.

2) From the results of the 3D scanning experiments, a symmetrical and glass-like density distribution can be clearly seen in the center of the scanning region where the density of the joint is higher than any other parts. From the top to the bottom view, it can be concluded that there exists an obvious stratified density distribution, which may have a close connection with the excellent mechanical performance of the *Zabelia biflora*.

3) One of the dynamic results firstly describes that the dynamic compression strength will decrease when the water content ascends at every strain rate. In detail, if the moisture content is below the fiber saturation point (11% - 12%), the compression strength will rise abruptly with the decrease of the moisture content when the strain rate is less than 3000 s^{-1}, otherwise, this enhancement will be slower. Secondly, the strain rate exerts a reinforcement effect on the compression strength when the moisture is kept unvaried. It is not until the strain rate has been improved exceeding 1000 s^{-1} that there will be a sudden drop in the stress after the first arrival of the compression strength. Lastly, the effect of the moisture content on the dynamic platform stress of the material matters only under low strain rates. Besides, once the moisture content exceeds the fiber saturation point, this effect will disappear.

ACKNOWLEDGEMENT

This work is funded by the National Natural Science Foundation of China (No.1230130, No 11521062 and No.11221202).

REFERENCES

1. Adler, D.C., Buehler, J., 2013: Mesoscale mechanics of wood cell walls under axial strain. Soft Matter 9: 7138-7144.
2. Allison, P.G., Chandler, M.Q., Rodriguez, R.I., Williams, B.A., Moser, R.D., 2013: Mechanical properties and structure of the biological multilayered material system Atractosteus spatula scales. Acta Biomater 9: 5289-5296.
3. Baño, V., Arriaga, F., Guaita, M., 2013: Determination of the influence of size and position of knots on load capacity and stress distribution in timber beams of *Pinus sylvestris* using finite element model. Biosystems Engineering 114(3): 214.
4. Borrega, M., Ahvenainen, P., Serimaa, R., Gibson, L.J., 2015: Composition and structure of balsa (*Ochroma pyramidale*) wood. Wood Science and Technology 49: 403- 420.
5. Buksnowitz, C., Hackspiel, C., Hofstetter, K., Müller, U., Gindl, W., Teischinger, A., Konnerth, J., 2010: Knots in trees: strain distribution in a naturally optimised structure. Wood Science & Technology 44(3): 389.
6. Caré, S., Bornert, M., Bertrand, F., Lenoir, N., 2012: 15th International Conference on Experimental Mechanics. Jul 2012, Porto, Portugal. Durabilité des assemblages collés.

7. Dimas, L.S., Bratzel, G.H., Eylon, I., Buehler, M.J., 2013: Tough composites inspired by mineralized natural materials: Computation, 3D printing, and testing. Advanced Functional Materials 23: 4629-4638.
8. Duigou, A.L., Castro, M., Bevan, R., Martin, N., 2016: 3D printing of wood fibre biocomposites: From mechanical to actuation functionality. Materials & Design 96: 106-114.
9. Foley, C., 2003: Modeling the effects of knots in Structural Timber. Report TVBK-1027. Dissertation, Lund University, Sweden.
10. Fratzl, P., Weinkamer, R., 2007: Nature's hierarchical materials. Progress in Materials Science 52: 1263-1334.
11. Gao, H., Ji, B., Jager, I.L., Arzt, E., Fratzl, P., 2003: Materials become insensitive to flaws at nanoscale: lessons from nature. Proceedings of the National Academy of Sciences of the United States of America 100: 5597-5600.
12. Gordon, Jeronimidis, Richardson, 1980: Composites with high work of fracture [and Discussion]. Philosophical Transactions of the Royal Society of London 294: 545-550.
13. Gu, X.G., Su, I., Sharma, S., Voros, J., Qin, Z., Buehler, M.J., 2016: Three-dimensional-printing of bio-inspired composites. Journal of Biomechanical Engineering 138(2): 0210061-02100616.
14. Goodrich, T., Nawaz, N., Feih, S., Lattimer, D.Y., Mouritz, A.P., 2010: High-temperature mechanical properties and thermal recovery of balsa wood. Journal of Wood Science 56(6): 437-443.
15. Jacobs, B., Geuten, K., Pyck , N., Huysmans, S., Jansen, S., Smets, E., 2011: Unraveling the phylogeny of Heptacodium and *Zabelia* (Caprifoliaceae): An interdisciplinary approach. Syst. Bot. 36(1): 231-252.
16. Jeronimidis, G., 1980: The Fracture behaviour of wood and the relations between toughness and morphology. Proceedings of the Royal Society of London 208: 447-460.
17. Kránitz, K., Deublein, M., Niemz, P., 2014: Determination of dynamic elastic moduli and shear moduli of aged wood by means of ultrasonic devices. Materials & Structures 47(6): 925-936.
18. Mayo, S.C., Chen, F., Evans, R., 2010: Micron-scale 3D imaging of wood and plant microstructure using high-resolution X-ray phase-contrast microtomography. J. Struct. Biol. 171: 182-188.
19. Ogata, K., 1991: Wood anatomy of *Zabelia* (Caprifoliaceae) - Evidence for Generic Recognition. Iawa Bull 12: 111-121.
20. Oloyede, A., Groombridge, P., 2000: The influence of microwave heating on the mechanical properties of wood. J. Mater. Process. Tech. 100(1-3): 67-73.
21. Pan, N., 2014: Exploring the significance of structural hierarchy in material systems - A review. Applied Physics Reviews 1(2): 021302.
22. Park, Y.B., Lee, C.M., Koo, B.-W., Park, S., Cosgrove, D.J., Kim, S.H., 2013: Monitoring meso-scale ordering of cellulose in intact plant cell walls using sum frequency generation spectroscopy. Plant physiology 163: 907-913.
23. Ritchie, R.O., 2011: The conflicts between strength and toughness. Nature Materials 10: 817-822.
24. Reiterer, A., Lichtenegger, H., Tschegg, S., Fratzl, P., 1999: Experimental evidence for a mechanical function of the cellulose microfibril angle in wood cell walls. Philosophical Magazine A 79: 2173-2184.

25. Roszyk, E., Moliński, W., Fabisiak, E., 2013: Radial variation of mechanical properties of pine wood (*Pinus sylvestris* L.) determined upon tensile stress. Wood Research 58(3): 329-342.
26. Renaud, M., Rueff, M., Rocaboy, A.C., 1996: Mechanical behaviour of saturated wood under compression. Wood Science & Technology 30(3): 153-164.
27. Reid, S.R., Peng, C., 1997: Dynamic uniaxial crushing of wood, International Journal of Impact Engineerig. 19: 531-570.
28. Müller, Joščák, Teischinger, 2003: Strength of dried and re-moistened spruce wood compared to native wood. Holz als Roh- und Werkstoff 61: 439-443.
29. Sakellariou, A., Sawkins, T.J., Senden, T.J., Limaye, A., 2004: X-ray tomography for mesoscale physics applications. Physica A: Statistical Mechanics and its Applications 339: 152-158.
30. Startsev, O.V., Makhonkov, A., Erofeev, V., Gudojnikov, S., 2015: Impact of moisture content on dynamic mechanical properties and transition temperatures of wood. Journal Wood Material Science & Engineering 12(1): 55-62
31. Sun, J., Bhushan, B., 2012: Hierarchical structure and mechanical properties of nacre: a review. RSC Advances 2: 7617-7632.
32. Tsuchikawa, S., Kobori, H., 2015: A review of recent application of near infrared spectroscopy to wood science and technology. Journal of Wood Science 61: 213-220.
33. Vural, M., Ravichandran, G., 2003: Dynamic response and energy dissipation characteristics of balsa wood: experiment and analysis. International Journal of Solids and Structures 40(9): 2147-2170.
34. Wegst, U.G., Bai, H., Saiz, E., Tomsia, A.P., Ritchie, R.O., 2014: Bioinspired structural materials. Nature Materials 14(1): 23-36.

Liangfei Gong, *Qingming Zhang, Haozhe Liang, Siyuan Ren
Beijing Institute of Technology
State Key Laboratory of Explosion Science and Technology
Beijing 100081
China
*Corresponding author: qmzhang@bit.edu.cn

Qingming Zhang, Jie Wang
Beijing Institute of Technology
Department of Mechanics
School of Aerospace Engineering
Beijing 100081
China